Structure of Duplex Oxide Layer in Porous Alumina Studied by ^{27}Al MAS and MQMAS NMR

Takahiro Iijima,* Seiichi Kato, Ryuichi Ikeda, Shinobu Ohki, Giyuu Kido,
Masataka Tansho, and Tadashi Shimizu
National Institute for Materials Science, Tsukuba, 305-0003

(Received June 24, 2005; CL-050814)

A local structure analysis using ^{27}Al multiple-quantum magic-angle-spinning (MQMAS) and MAS NMR techniques has been performed on porous alumina fabricated by the anodic oxidation of aluminum. It is suggested that the main constituents of the inner and outer oxide layers composing porous alumina are [AlO_4 and AlO_5] and [AlO_6], respectively, and that both of the layers adopt the amorphous structure.

In recent years, porous alumina having uniform pores has attracted much interest in many fields.[1–4] Since the size, depth, and interval of the pores are highly controllable in the porous alumina materials fabricated by an anodic oxidation method, the application of them extends to accurate filters, catalyst supports, nanocomposites, photonic crystals, and so on. The structure of porous alumina has been proposed to be an assembly of a hexagonal column with the pore in its center by Keller and co-workers in 1953.[1] Thompson and Wood have reported that porous alumina consists of duplex oxide layers;[2] outer oxide layer existing adjacent to the pore is composed of anion-incorporated alumina, whereas inner layer existing remote from it is of pure alumina. The inhomogeneous distribution of the anionic species concentrated in the intermediate part of the outer oxide has been suggested in order to account for the nonuniform refractive index observed.[3] However, the structure of alumina in each oxide layer has not been clarified yet, although such information is essential when the material having nanofunction is designed. This can be due to the amorphous structure of porous alumina that is reported for the material synthesized by a sol–gel method.[5]

High-resolution solid-state NMR is a powerful tool for analyzing the local structure of both crystalline and noncrystalline materials.[6] For example, diffraction experiments are unable to provide detailed information about the local structure for the amorphous sample, while NMR remains sensitive to local bonding parameters. In particular, ^{27}Al ($S = 5/2$) magic-angle spinning (MAS) NMR that can distinguish the coordination environment around it has been ubiquitously used for the structural characterization of the inorganic materials. Further detailed structural information around ^{27}Al nuclei is obtainable from a two dimensional NMR method of multiple-quantum MAS (MQMAS) developed by Frydman and co-workers in 1995 for acquiring the high-resolution spectrum of half-integer quadrupole nuclei.[7] In the present work, the local structure of porous alumina fabricated by the anodic oxidation is investigated by using ^{27}Al MAS and MQMAS NMR spectra. We will discuss the structure of both oxide layers by analyzing the obtained ^{27}Al NMR spectra.

Three samples of porous alumina were prepared by the anodic oxidation; 99.99% aluminum sheets were oxidized in 0.3 M sulfuric acid at 22 V (**A**), 0.3 M oxalic acid at 40 V (**B**), and 0.3 M phosphoric acid at 130 V (**C**). Scanning electron micrograph (SEM) was measured for the obtained membranes of porous alumina using a JEOL JSM-6500 FEG-SEM. The ^{27}Al MAS and MQMAS NMR spectra were recorded at 21.9 T on a JEOL ECA 930 spectrometer equipped with a JEOL 4 mm MAS probe. The ^{27}Al resonant frequency was 242.398 MHz. The MAS frequency of $\nu_r = 18$ kHz was stabilized within ± 10 Hz by a JEOL MAS speed controller. The ^{27}Al chemical shift is referenced to 1.0 M $AlCl_3$ solution at -0.1 ppm. Three pulse sequence employing z-filter[8] was used for acquiring the triple-quantum (3Q) MAS NMR spectrum.

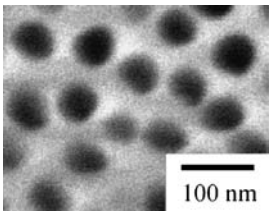

Figure 1. Scanning electron micrograph of porous alumina fabricated by anodic oxidation using oxalic acid.

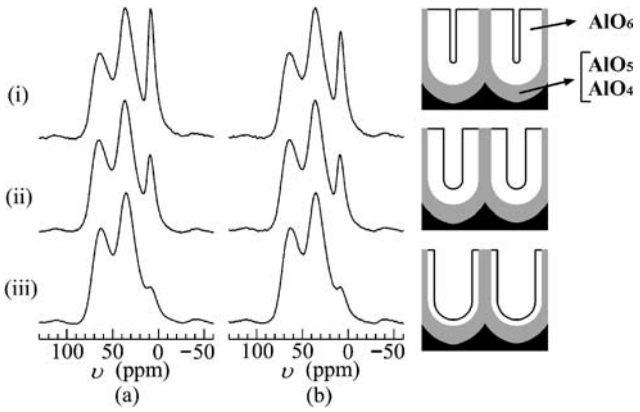

Figure 2. ^{27}Al MAS NMR spectra of the powder sample of porous alumina synthesized using (i) sulfuric, (ii) oxalic, and (iii) phosphoric acids. (a) and (b) show the spectra for the samples without and with drying, respectively. The 20° pulse of the width $p_w = 0.9$ μs with the irradiation frequency $\nu_1 = 31$ kHz was used. The side view of porous alumina consisting of the duplex oxide layers is schematically shown on the right side of the spectra. The black, gray, and white areas represent aluminum metal, inner oxide and outer oxide, respectively.

Figure 1 shows the top view of the SEM image of porous alumina of the sample (**B**). The black spots in this picture represent the pore of porous alumina. The SEM images of two other samples were similarly obtained. We estimated the diameters of the pore of porous alumina (**A**), (**B**), and (**C**) as ca. 10, 50, and 150 nm, respectively.

Figure 2(a) shows the ^{27}Al MAS NMR spectra of the powder

samples of porous alumina (**A**), (**B**), and (**C**). Each of these spectra consists of three broad peaks positioned at 66, 38, and 9 ppm, which can be assigned to four- (AlO_4), five- (AlO_5), and six-fold (AlO_6) oxygen-coordinated aluminum atoms, respectively.[5] The spectra are normalized to the peak of ^{27}Al in AlO_5. The significant fraction of AlO_5 has been also detected for porous alumina and related materials fabricated by the sol–gel method.[5,9] The pore size dependence of the spectrum can be clearly seen for the peak of ^{27}Al in AlO_6. The relative intensity of ^{27}Al in AlO_4 was 0.70 ± 0.04 for the three samples, whereas that in AlO_6 was 0.99, 0.58, and 0.29 for the samples (**A**), (**B**), and (**C**), respectively. The correlation between the pore size and the duplex oxide structure has been already reported;[3] increasing the pore diameter accompanies the decrease of the thickness of the outer oxide layer, leaving that of the inner oxide layer unchanged, as drawn schematically on the right side of the spectra in Figure 2. Therefore, we propose that the outer oxide layer is mainly composed of AlO_6, while the inner one is AlO_4 and AlO_5. The AlO_6-rich structure of the outer layer is reasonable, because the outer oxide contacts the electrolysis solution during the synthesis and water molecules can easily bond to the aluminum atoms. Figure 2b shows the ^{27}Al MAS spectra for the dried samples. The relative intensity of ^{27}Al in AlO_6 for the sample (**A**) having the thickest outer oxide layer decreased from 0.99 to 0.83 by the drying. This indicates that some of the water molecules in the outer layer are removed by the drying and that the coordination number of aluminum decreased from six to four or five.

Figure 3 shows the ^{27}Al 3QMAS spectrum of the powder sample of porous alumina (**B**). The 3QMAS spectra for two other samples were almost the same except for the peak height of ^{27}Al in AlO_6. F_1 and F_2 axes represent the isotropic and MAS axes of ^{27}Al, respectively. The projection of the MQMAS spectrum onto the F_2 axis corresponds to the ^{27}Al MAS NMR spectrum, while that onto the F_1 axis to the ^{27}Al high-resolution spectrum

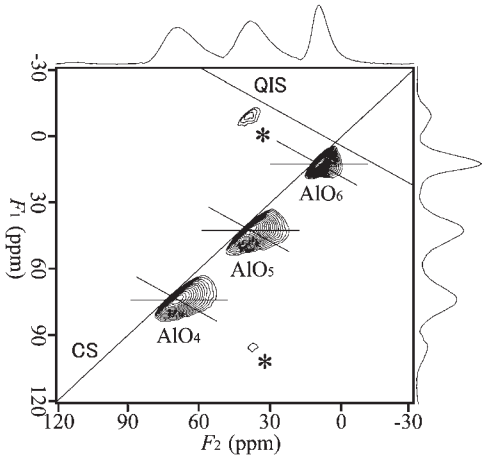

Figure 3. ^{27}Al 3QMAS NMR spectrum of the powder sample of porous alumina synthesized using oxalic acid and projections to F_1 (isotropic) and F_2 (MAS) dimensions. The peaks marked by * show the spinning side bands of the main peak. CS and QIS represent the chemical shift and quadrupole-induced shift axes, respectively. The lines parallel to F_2 and QIS axes are also shown for each peak. The pulse parameters were (ν_1, p_w) of (150 kHz, 2.8 μs) for the first pulse exciting triple-quantum coherence, (150 kHz, 1.0 μs) for the second pulse converting to zero-quantum coherence, and (14 kHz, 15 μs) for the final pulse generating single-quantum coherence.

free from the broadening due to the second-order quadrupole coupling (SOQC). The asymmetric structure especially for the peaks of ^{27}Al in AlO_4 and AlO_5 in F_2-projected spectrum is caused by the SOQC, which becomes symmetric one in F_1-projected spectrum. The NMR parameters of the isotropic chemical shift δ and quadrupole product $P_Q = e^2Qqh^{-1}(1 + \eta^2/3)^{1/2}$, where e^2Qqh^{-1} and η are the quadrupole coupling constant and asymmetric parameter, respectively, can be estimated from the peak position of the MQMAS spectrum.[7,10] The values of (δ, P_Q) for ^{27}Al in AlO_4, AlO_5, and AlO_6 are obtained as (72.2 ppm, 4.3 MHz), (41.0 ppm, 4.1 MHz), and (11.2 ppm, 3.2 MHz), respectively. When the δ and P_Q values are distributed owing to the amorphous structure, the peak of the MQMAS spectrum elongates along the chemical shift (CS) and quadrupole-induced shift (QIS) axes, respectively. Since all of three ^{27}Al peaks are elongated along CS axis, both of the inner and outer oxide layers are revealed to be amorphous. The distribution of the δ value may be caused by that of the Al–O–Al bond angle.[11] On the other hand, the distribution of the P_Q value is different among the three ^{27}Al species. The peaks of ^{27}Al in AlO_4 and AlO_5 are elongated along F_2 axis rather than QIS axis. The P_Q value of ^{27}Al is determined by a tensor of the electric field gradient made by the atomic group surrounding ^{27}Al. Since the inner oxide layer consists of the pure alumina,[2,3] the P_Q value is mainly dominated by the symmetry of the polyhedron of AlO_4 and AlO_5, and thus the distribution of the distortion of them seems to be relatively small. The peak for AlO_6 elongated largely along QIS axis shows that the electric field gradient is considerably distributed. Such a distribution is caused by the random distortion of AlO_6 and/or the anions incorporated inhomogeneously in the outer oxide layer. Finally, we note that the line width of F_1-projected spectrum for ^{27}Al in AlO_6 is smaller than that in AlO_4 and AlO_5, which is caused by the degree of the distribution of the δ value for each ^{27}Al species.

In summary, we have measured the ^{27}Al MAS and MQMAS spectra of porous alumina in order to clarify the local structure of it. Such structure has not been analyzed so far by any methods other than NMR, which can be due to the amorphous structure. It is suggested that the oxides in the inner and outer layers of porous alumina are mainly composed of [AlO_4 and AlO_5] and [AlO_6], respectively, and that the structures of both layers are amorphous.

References

1 F. Keller, M. S. Hunter, and D. L. Robinson, *J. Electrochem. Soc.*, **100**, 411 (1953).
2 G. E. Thompson and G. C. Wood, *Nature*, **290**, 230 (1981).
3 J. Choi, Y. Luo, R. B. Wehrspohn, R. Hillebrand, J. Schilling, and U. Gosele, *J. Appl. Phys.*, **94**, 4757 (2003).
4 H. Masuda and K. Fukuda, *Science*, **268**, 1466 (1995).
5 L. Wilcox, G. Burnside, B. Kiranga, R. Shekhawat, M. K. Mazumder, R. M. Hawk, D. A. Lindguist, and S. D. Burton, *Chem. Mater.*, **15**, 51 (2003).
6 K. Schmidt-Rohr and H. W. Spiess, "Multidimensional Solid-State NMR and Polymers," Academic Press, London (1994).
7 L. Frydman and J. S. Harwood, *J. Am. Chem. Soc.*, **117**, 5367 (1995); A. L. Medek, J. S. Harwood, and L. Frydman, *J. Am. Chem. Soc.*, **117**, 12779 (1995).
8 J.-P. Amoureux, C. Fernandez, and S. Steuernagel, *J. Magn. Reson., Ser. A*, **123**, 116 (1996).
9 D. Coster and J. J. Fripiat, *Chem. Mater.*, **5**, 1204 (1993).
10 J.-P. Amoureux and C. Fernandez, *Solid State Nucl. Magn. Reson.*, **10**, 211 (1998); A. Goldbourt and P. K. Madhu, *Monatsh. Chem.*, **133**, 1497 (2002).
11 D. Muller, E. Jahn, G. Ludwig, and U. Haubenreisser, *Chem. Phys. Lett.*, **109**, 332 (1984).

Published on the web (Advance View) August 20, 2005; DOI 10.1246/cl.2005.1286